THE JOURNAL OF BIOLOGICAL CHEMISTRY
Vol. 278, No. 27, Issue of July 4, pp. 24837–24848, 2003
Printed in U.S.A.

An Ancestral Secretory Apparatus in the Protozoan Parasite *Giardia intestinalis**

Received for publication, February 27, 2003, and in revised form, April 23, 2003
Published, JBC Papers in Press, April 23, 2003, DOI 10.1074/jbc.M302082200

Matthias Marti, Attila Regös, Yajie Li‡, Elisabeth M. Schraner§, Peter Wild§, Norbert Müller¶, Lea G. Knopf, and Adrian B. Hehl‖**

From the Institute of Parasitology, University of Zürich, CH-8057 Zürich, Switzerland, the §Electron Microscopy Unit, Institutes of Veterinary Anatomy and Virology, University of Zürich, CH-8057 Zürich, Switzerland, and the ¶Institute of Parasitology, University of Bern, CH-3012 Bern, Switzerland

The protozoan parasite *Giardia intestinalis* belongs to one of the earliest diverged eukaryotic lineages. This is also reflected in a simple intracellular organization, as *Giardia* lacks common subcellular compartments such as mitochondria, peroxisomes, and apparently also a Golgi apparatus. During encystation, developmentally regulated formation of large secretory compartments containing cyst wall material occurs. Despite the lack of any morphological similarities, these encystation-specific vesicles (ESVs) show several biochemical characteristics of maturing Golgi cisternae. Previous studies suggested that Golgi structure and function are induced only during encystation in *Giardia*, giving rise to the hypothesis that ESVs, as a *Giardia* Golgi equivalent, are generated *de novo*. Alternatively, ESV compartments could be built on the template structure of a cryptic Golgi in trophozoites in response to ER export of cyst wall material during encystation. We addressed this question by defining the molecular framework of the *Giardia* secretory apparatus using a comparative genomic approach. Analysis of the corresponding transcriptome during growth and encystation revealed surprisingly little stage-specific regulation. A panel of antibodies was generated against selected marker proteins to investigate the developmental dynamics of the endomembrane system. We show evidence that *Giardia* accommodates the export of large amounts of cyst wall material through re-organization of membrane compartment(s) in trophozoites with biochemical similarities to ESVs. This suggests that ESVs are selectively stabilized Golgi-like compartments in a unique and archetypical secretory system, which arise from a structural template in trophozoites rather than being generated *de novo*.

Giardia intestinalis is a flagellated protist of the diplomonad group that commonly causes diarrheal disease throughout the world. All known free-living and parasitic diplomonads share some unique structural features, including the absence of mitochondria, peroxisomes, and a recognizable Golgi apparatus (1–3). These early observations and more recent phylogenetic studies (4, 5) supported the notion that the diplomonads are early diverged or "primitive" eukaryotes, despite the identification of a few genes of proteobacterial origin in the diplomonad species *G. intestinalis* (6, 7) and *Spironucleus barkhanus* (8).

Asexually dividing, motile trophozoite forms of *Giardia* colonize the upper intestine of vertebrate hosts, and are shed as environmentally resistant, infectious cysts. The intracellular organization of the binucleate trophozoite is unusually simple, also in comparison with other phylogenetically basal groups such as the trichomonads (*e.g. Trichomonas vaginalis* (9)) and the kinetoplastids (*e.g. Trypanosoma cruzi* (10)). A compartment with functional and structural characteristics of the endoplasmic reticulum (ER)[1] has been identified and characterized as an endomembraneous network, which extends throughout the cell body. Immunoelectron microscopy studies demonstrated the localization of giardial BiP (11), three protein-disulfide isomerase paralogues (12), as well as trophozoite and cyst surface antigens in the *Giardia* ER (13). Other morphologically recognizable membrane compartments are the peripheral vesicles (PVs, approximately 150–200 nm in size), which are thought to perform both lysosomal and endosomal activities (14). PVs underlie the plasma membrane of the cell body except at the flagella or where it covers the cytoskeleton structures of the ventral disk (14). A third intracellular compartment, encystation-specific vesicles (ESVs) (15), arises only during the highly orchestrated process of encystation. Formation and maturation of the large ESVs (up to 1 μm diameter) is functionally linked to the regulated expression of exported cargo (*i.e.* cyst wall proteins), and there is increasing evidence that ESVs may be the cisternae of a unique Golgi equivalent in *Giardia* (16–18). We recently demonstrated that sorting of

* This work was supported in part by Swiss National Science Foundation Grants 31-58912.99 and 31-100270/1, the Novartis Foundation, and the "Stiftung für wissenschaftliche Forschung an der Universität Zürich." The costs of publication of this article were defrayed in part by the payment of page charges. This article must therefore be hereby marked "*advertisement*" in accordance with 18 U.S.C. Section 1734 solely to indicate this fact.

The nucleotide sequence(s) reported in this paper has been submitted to the GenBank™/EBI Data Bank with accession number(s) AF503489, AF503488, AF486294, AF486293, AY078979, AY078978, AY078976, AY078977, AF456417, AF456415, AF481768, AF481767, AF481766, AF481765, AF456416, and AY219652.

S The on-line version of this article (available at http://www.jbc.org) contains tables.

‡ Supported by a training grant from the China Scholarship Council. Present address: Dept. of Parasitology, Harbin Medical University, 150086, Harbin, Peoples Republic of China.

‖ To whom correspondence should be addressed. Institute of Parasitology, University of Zürich, Winterthurerstrasse 266a, CH-8057 Zürich, Switzerland. Tel.: 41-1-635-8526; Fax: 41-1-635-8907; E-mail: ahehl@vetparas.unizh.ch.

** Present address: Division of Infection and Immunity, The Walter and Eliza Hall Institute of Medical Research, Parkville, Victoria 3050, Australia.

[1] The abbreviations used are: ER, endoplasmic reticulum; PV, peripheral vesicle; ESV, encystation-specific vesicles; RT, reverse transcriptase; ORF, open reading frame; MBP, maltose-binding protein; PBS, phosphate-buffered saline; mAb, monoclonal antibody; pAb, polyclonal antibody; FITC, fluorescein isothiocyanate; AP, adapter protein; TGN, trans Golgi network; PP2, protein phosphatase 2; ARF, ADP-ribosylation factor; IFA, immunofluorescence assay.

exported proteins to the regulated secretory pathway via ESVs or a second constitutively active export pathway to the plasma membrane occurred at or immediately after ER exit (18). This also argued for the absence of a conventional Golgi apparatus in all developmental stages. Thus, current data suggests the presence of a primordial secretory system in *Giardia*, but very little is known about its molecular characteristics. Here we report a broad approach to analyze the functional anatomy of this unusual and dynamic membrane system and to investigate its putatively ancestral nature. Specifically, we addressed the question whether the cellular machinery for the generation of the Golgi-like ESV compartments indeed arises *de novo* during encystation, or whether a functional, or even a morphologically identifiable Golgi equivalent is present in trophozoites that could be used as a template on which encysting cells build ESVs. We established a molecular framework for secretory transport in this ancient eukaryote using a comparative genomics approach and provide evidence for the presence of membrane compartments with Golgi characteristics in trophozoites as well. Despite significant morphological changes, there is little evidence for regulation on a molecular level, indicating that generation of ESVs as a stabilized Golgi equivalent in *Giardia* is achieved in large part though re-organization of constitutive elements of this secretory system.

EXPERIMENTAL PROCEDURES

Cell Culture—Trophozoites of *Giardia* strains WBC6 (ATCC number 50803) were grown vegetatively in TYI-S-33, supplemented with 10% of adult bovine serum and bovine bile. Cells were *in vitro* encysted according to the two-step method described by Boucher and Gillin (19). Cells were harvested by chilling culture tubes on ice for 30 min, inverting 10 times, and collection of cells by centrifugation at 800 × *g*.

Identification of Giardia Genes and Sequence Confirmation—Each putative *Giardia* orthologue was identified individually using the online tBLASTN[2] tool to search *Giardia* HTGS sequences (20). The genome coverage as of April 2002 was 7.3-fold with an estimated 98.3% of the sequence determined.[3] Contigs of assembled single-pass reads were manually scanned for the AT-rich region immediately preceding a translation start codon and the consensus *Giardia* polyadenylation signal AGTPurAAPyr at, or shortly after the stop codon. Identities of putative ORFs were confirmed using the BLASTP tool, and e-values and GenBank™ accession numbers of best hits were determined (see also Table I). Conserved domains were used to further confirm tentative identifications with the Pfam tool[4] using default parameters. Predictions of transmembrane domains and prenylation motifs were performed using PSORTII.[5]

Semi-quantitative RT-PCR—Total RNA from 5×10^6 trophozoites or encysting cells (3, 7, 15, and 24 h after induction of encystation) was prepared using the Stratagene total RNA kit (Stratagene, La Jolla, CA) following digestion with 30 units of DNase for 15 min at 37 °C. For first strand cDNA synthesis, 3.5 μg of total RNA were reverse-transcribed with 100 ng of primer k-anchor and 50 units of SuperScript II reverse transcriptase (Invitrogen, Carlsbad, CA) at 45 °C in 25 mM Tris-HCl, pH 8.3, 75 mM KCl, 3 mM $MgCl_2$, 10 mM dithiothreitol, and 500 μM dNTP (Clontech, Palo Alto, CA). The reaction was incubated at 45 °C for 50 min and heat inactivated at 70 °C followed by digestion with 10 units of RNase H for 20 min at 37 °C. Single-stranded cDNA was purified with the Concert DNA purification spin cartridge system (Invitrogen). Single-stranded cDNA corresponding to 70 ng of total RNA was used as template for semi-quantitative PCR analysis with 8 pmol each of primer k-adaptor and a gene-specific primer. A list of all primers used for RT-PCR and semi-quantitative PCR is available as Supplementary Material. Primer sequences were chosen to amplify fragments between 100 and 500 bp, containing the end of the gene ORF and the complete 3′-untranslated region. Reaction conditions were 10 mM Tris-HCl, pH 8.3, 50 mM KCl, 2 mM $MgCl_2$, 200 μM each dNTP, and 1 unit of recombinant *Taq* polymerase (Sigma). Thermal cycling conditions were as follows: "hot start cycle," 94 °C for 5 min, 80 °C for 2 min (addition of *Taq* polymerase), 64 °C for 30 s, 72 °C for 30 s, followed by 22–32 cycles (depending on the copy number of a specific cDNA) at 94 °C for 30 s, 64 °C for 30 s, and 72 °C for 30 s. PCR products were separated on a 1.5% agarose gel containing 0.01% SYBR Green I (Molecular Probes, Eugene, OR). Data collection was performed on a fluorimager (Alpha Innotech Corp., San Leandro, CA) using ChemiImager 5500 software. For all the cDNA products, the log-linear range was between 20 and 30 PCR cycles. Negative controls included: 1) omission of cDNA template in the PCR reaction and 2) omission of enzyme in the RT reaction.

Expression and Purification of Bacterial Fusion Proteins—The nucleotide sequences encoding amino acids 10–170 of *Giβ′COP*, 8–189 of *GiSar1p*, 430–705 of *GiCLH*, 25–176 of *GiRab11*, 97–270 of *GiSyn1*, as well as 8–201 and 344–714 of *GiDLP* and 3–111 of *GiYip* were PCR amplified from genomic DNA and subcloned into the polylinker region of the pMal-2Cx expression vector (New England Biolabs), downstream of the maltose-binding protein (*MBP*) gene, giving rise to fusion genes *MBP-Giβ′COP*, *MBP-GiSar1p*, *MBP-GiCLH*, *MBP-GiRab11*, *MBP-GiSyn1*, *MBP-GiDLPn*, and *MBP-GiDLPc* (corresponding to N- and C-terminal fragments of GiDLP, respectively), and *MBP-GiYip*. Bacterial overexpression of fusion proteins was induced by adding 0.5 mM isopropyl-β-D-thiogalactopyranoside for 2 h at 37 °C, and fusion proteins were affinity purified from bacterial cold shock lysates on amylose resin according to manufacturers protocols and lyophilized as previously described (21). Primers used for the amplification of marker gene fragments are available as Supplementary Material.

Peptide Synthesis—Synthesis of a polypeptide for antibody production was performed by Eurogentec (Seraing, Belgium). A peptide corresponding to Glu-613 through Lys-630 of the GiDLP protein, NH_2C-ESVPEKIKAQGPLSEAEK-COOH, was synthesized and coupled to keyhole limpet hemocyanin.

Production of Polyclonal Antibodies—BALB/c mice were immunized intraperitoneally on days 0, 15, and 30 with ~50 μg of fusion protein or 10 μg of keyhole limpet hemocyanin-coupled peptide resuspended in 100 μl of phosphate-buffered saline (PBS) and emulsified with an equal volume of RIBI adjuvant (Corixa, Hamilton MT). Blood was collected prior to initial immunization and after each boost from the tail vein, the serum fraction was assayed for specific antibody content.

SDS-PAGE and Immunoblotting—Cells were harvested as described above, cell pellets were washed once in ice-cold PBS and counted. SDS sample buffer was added to obtain a uniform concentration of 5×10^5 cells per sample, and samples were immediately boiled for 3 min. 10% Polyacrylamide gels were run under reducing conditions with 7.75 mg/ml dithiothreitol in samples, and proteins were transferred to a nitrocellulose membrane according to standard methods. Antisera were diluted as specified below in PBS, 0.05% Tween 20, and 5% nonfat milk powder. CWP2 was detected with mouse mAb 7D2 (22) and diluted 1:20,000. Mouse pAbs raised against *Giardia* marker proteins GiSar1p, Giβ′COP, GiCLH, GiSyn1, and GiYip1p were diluted 1:1000, and to GiCLH and GiDLP 1:5000. Primary antibodies were detected with a peroxidase-conjugated rabbit anti-mouse or goat anti-rabbit antibody (both Sigma), respectively, and visualized using the ECL system (PerkinElmer Life Sciences).

Immunofluorescence Microscopy—All manipulations were carried out at 4 °C. Trophozoites and encysting cells were harvested as described above, washed twice in ice-cold PBS, and fixed with 3% paraformaldehyde for 30 min at room temperature, followed by a 5-min incubation with 100 mM glycine in PBS. Fixed cells were permeabilized with 0.1% Triton X-100 in PBS for 30 min and blocked >1 h in 2% bovine serum albumin in PBS. Fixed and permeabilized cells were incubated with primary antibodies diluted in 2% bovine serum albumin, 0.1% Triton X-100% in PBS for 1 h. Mouse polyclonal antibodies have been diluted 1:200 (except GiDLPn and GiCLH, these pAbs were diluted 1:1000), and Texas Red-conjugated mouse mAb A300-TR (Waterborne, New Orleans, LA), an anti-CWP antibody, 1:30. After washing with ice-cold PBS, cells were incubated for 1 h with FITC-conjugated sheep anti-mouse antibody (Sigma). Fluorescence microscopy was performed on a Leica DM-IRBE microscope using a ×100 HCX PL Fluotar lens (Leica Microsystems GmbH, Wetzlar, Germany) and digital images were recorded using a cooled CCD camera (Diagnostic Instruments Inc.) and processed with the Metaview software package (Visitron Systems GmbH, Puchheim, Germany).

Electron Microscopy—Trophozoites or encysting cells were cultivated as described above. After collection, cells were washed twice in ice-cold PBS and transferred into 6-well plates containing 10–12 sapphire glasses per well in pre-warmed PBS (37 °C). To promote attachment to these 30-μm thick carbon-coated sapphire disks, cells were then incubated at room temperature for 5 min. Sapphire disks covered with a monolayer of attached parasites were subsequently plunged into a

[2] www.ncbi.nlm.nih.gov/blast.
[3] jbpc.mbl.edu/Giardia-HTML/summary.html.
[4] www.sanger.ac.uk./cgi-bin/Pfam/nph-search.cgi.
[5] psort.nibb.ac.jp.

mixture of liquid propane/ethane (8/2) cooled by liquid nitrogen using a custom device. The ultra-rapidly frozen samples were substituted at −90 °C in acetone containing 0.5% osmium tetroxide and 0.25% glutaraldehyde (23) overnight. The temperature was then continuously (5 °C/h) raised to 0 °C, and the samples embedded in Epon at 4 °C. After polymerization at 60 °C for 2 days, ultrathin sections were cut parallel to the sapphire surface, stained with uranyl acetate and lead citrate, and examined in a CM 12 electron microscope (Philips, Netherlands) equipped with a slow scan CCD camera (Gatan, Pleasanton, CA) at an acceleration voltage of 100 kV. Recorded pictures have been processed with the Digital micrograph 3.34 software (Gatan).

Sucrose Density Gradient Centrifugation and Subcellular Fractionation—All manipulations were carried out at 4 °C. Cells were grown at 37 °C in triple surface flasks (Nunc, Roskilde, Denmark) to a density of approximately 1×10^9 cells/flask, harvested as described above, and washed once in ice-cold PBS. For quantitative assays (densitometric quantification, biochemical assays), cell numbers of different populations (trophozoites and encysting cells) were normalized after determining the absolute cell number with a Neubauer chamber. The adjusted cell pellet was then resuspended in 4 ml of ice-cold PBS containing a 2× protease inhibitor mixture (1 mM 4-(2-aminoethyl)benzenesulfonyl fluoride, 1 mM EDTA, 2 μM E-64, 2 μM leupeptin, and 300 nM aprotinin; Calbiochem, San Diego, CA) and 1 mM phenylmethylsulfonyl fluoride. This suspension was transferred into a 15-ml Falcon tube (BD Biosciences, Franklin Lakes, NJ) and processed on a fixed stand with a sonifier (Branson, Danbury, CT) using a total of 5 pulses of 30 s each (setting 2, 10% pulse intensity). Microscopic examination was used to confirm that trophozoites and encysting cells (but not cysts) were completely disintegrated. After adding sucrose to a final concentration of 250 mM, the suspension was centrifuged for 10 min at 1000 × *g* and the supernatant harvested. 1.8 ml of this postnuclear supernatant were layered onto a discontinuous sucrose gradient in 12-ml polyallomer tubes (Beckman-Spinco) made from four 0.5-ml layers of 60, 55, 50, and 45% sucrose and five 1.5-ml layers of 40, 35, 30, 25, and 20% sucrose, which resulted in a total volume of 11.3 ml including the loaded cell suspension sample. This discontinuous sucrose gradient was centrifuged at 100,000 × *g* for 18 h at 4 °C. The gradient was eluted from the bottom into 18 fractions of 600 μl each, and stored as 300-μl aliquots at −20 °C for further analysis or directly processed for biochemical assays (see below). Protein content in each fraction was measured with the BCA protein assay kit (Pierce). For SDS-PAGE, aliquots were further diluted with PBS to 1 ml, and proteins were precipitated by addition of 250 μl of concentrated trichloroacetic acid. Precipitated proteins were collected by centrifugation at 10,000 × *g* for 10 min, washed once with acetone, and air dried for 1 h at room temperature. Dried and washed protein pellets were redissolved in 100 μl of SDS-PAGE sample buffer containing 7.75 mg/ml dithiothreitol, boiled for 3 min, loaded on a 10% SDS-PAGE gel, and processed for Western analysis as described above. The Western data have been analyzed densitometrically using Chemi-Imager 5500 software (Alpha Innotech, San Leandro, CA) and are indicated relative (in %) to the maximum value (100%). Protein content (indicated in μg/ml) was determined for each fraction in both developmental stages, and CWP2 was used as an internal marker for ESV localization. In addition, the activity of the usually Golgi-specific enzyme GlcNAc-transferase was measured in both developmental stages (see below).

Glycosyltransferase Assay—*N*-Acetylglucosamine transferase activity assay was performed essentially as described by Vischer and Hughes (24). Briefly, 300-μl aliquots of each subcellular fraction were diluted with an equal volume of assay buffer to a final concentration of 50 mM sodium phosphate, pH 6.9, 5 mM $MgCl_2$, 5 mM $MnCl_2$, 10 mM KCl, 0.1% Triton X-100, and 5 mM pyrophosphate. To saturate non-catalytic binding of substrate, samples were preincubated with 1 mM cold (unlabeled) UDP-*N*-acetylglucosamine and 2 mg of ovalbumin as a donor for 2 h at the restrictive temperature of 4 °C. The reaction was started by addition of labeled UDP-*N*-acetyl-[^{3}H]glucosamine (1.67 kBq per fraction) and shifting the temperature to 37 °C. After 1.5 h of incubation, the reaction was terminated with 1 ml of ice-cold 0.5 M HCl containing 1% phosphotungstic acid. The precipitates were collected by centrifugation and the pellet carefully resuspended in 1 ml of H_2O to completely resolve co-precipitated sugars, centrifuged, and incubated with 1 ml of ice-cold 95% ethanol for 5 min at 4 °C. Finally, precipitates were neutralized with 500 μl of 0.5 M NaOH overnight at room temperature and counted in 10 ml of scintillation mixture (PerkinElmer Life Sciences) on a liquid scintillation counter (PerkinElmer Life Sciences).

Nucleotide Sequence Accession Numbers—The sequence data used for (i) phylogenetic inferences of translated ORFs and/or (ii) for recombinant expression and antibody production have been confirmed by microsequencing (Microsynth GmbH, Balgach, Switzerland) and are available from EMBL/GenBank™/DDBJ under the following accession numbers: putative adaptor protein complex large chain subunit *BetaB* AF503489; putative adaptor protein complex large chain subunit *BetaA* AF503488; *G. intestinalis* γ-adaptin gene AF486294; *G. intestinalis* α-adaptin gene AF486293; putative adaptor protein complex medium subunit (*MuA*) AY078979; putative adaptor protein complex medium subunit (*MuB*) AY078978; putative adaptor protein complex small chain subunit (*SigmaA*) AY078976; putative adaptor protein complex small chain subunit (*SigmaB*) AY078977; putative coatomer protein complex I subunit gene AF456417; *G. intestinalis* t-SNARE-like protein (*SYN1*) AF456415; *G. intestinalis* strain WBC6 RabA (*RabA*) (*GiRabA*) AF481768; *G. intestinalis* strain WBC6 *RabB* (*GiRabB*) (RabB) AF481767; *G. intestinalis* strain WBC6 RabF (*RabF*) (*GiRabF*) AF481766; *G. intestinalis* strain WBC6 RabD (*RabD*) (*GiRabD*) AF481765; *G. intestinalis* dynamin-like protein (*GiDLP*) gene, with complete cds AF456416; *G. intestinalis Yip1* homologue (*GiYip*) *AY219652.*

RESULTS

A tEM Survey of the Giardia Membrane Compartment Morphology Reveals the Lack of a Recognizable Golgi Apparatus—The *Giardia* endomembrane system undergoes significant morphological changes during stage conversion, culminating in the emergence of large membrane-bound compartments containing cyst wall material (ESVs) and subsequent cyst wall assembly (15–17). Previous reports have described a Golgi apparatus structure (*i.e.* stacked cisternae) in encysting parasites and occasionally in proliferating trophozoites (11, 25). In contrast, more recent data suggested that ESVs corresponded to individual Golgi compartments, which mature *in situ* (18). All previous tEM studies had relied on analyzing randomly sectioned cells. Here we used a novel method to obtain uniformly oriented parasites sectioned in a dorso-ventral plane to determine whether a classical Golgi structure was present in these highly polarized cells, and to identify typical morphological features of the *Giardia* endomembrane system. The most prominent endomembrane compartments identified in trophozoites (Fig. 1*A*) were the nuclear envelope with the continuous extensive bilateral ER network (*small white arrowheads*), and the numerous peripheral vesicles underlying the plasma membrane (PV; *black arrowheads*). In parasites early after induction of encystation, we recently identified a limited number of discrete ER exit sites along the clamp-shaped ER indicating the presence of specific ER subdomains in *Giardia* (18). Additional gross changes of the compartment structure after induction of encystation were limited to the emergence of ESV compartments (Fig. 1*B*, *white arrows*) and a somewhat enlarged ER system. Most importantly, however, we were unable to confirm reports of stacked cisternae reminiscent of a typical eukaryotic Golgi apparatus, although we studied a large number of cells (>100 of each stage). The only membranes arranged in parallel were large spirals adjacent to, and probably continuous with, the nuclear envelope membranes (≤1.5 μm in diameter; *asterisks* in Fig. 1, *A* and *B*) common to all encysting cells and occasionally observed in proliferating trophozoites. Despite the lack of morphological conservation (*i.e.* stacks of flattened cisternae), ESVs therefore remained the only definable candidate Golgi equivalent in *Giardia* because of their biochemical properties.

The Molecular Basis for a Generic Eukaryotic Secretory System in Giardia—In a survey of the *Giardia* Genome Data base, we addressed the question whether this early diverged eukaryote harbors a classical secretory system despite its completely divergent morphology. Because most of the genes coding for key proteins involved in vesicular coating, budding, and fusion are members of gene families (26–28), the membrane compartment organization and complexity of a cell can be predicted by genomic approaches (26). We sought to define the molecular basis for *Giardia* secretory transport by a systematic

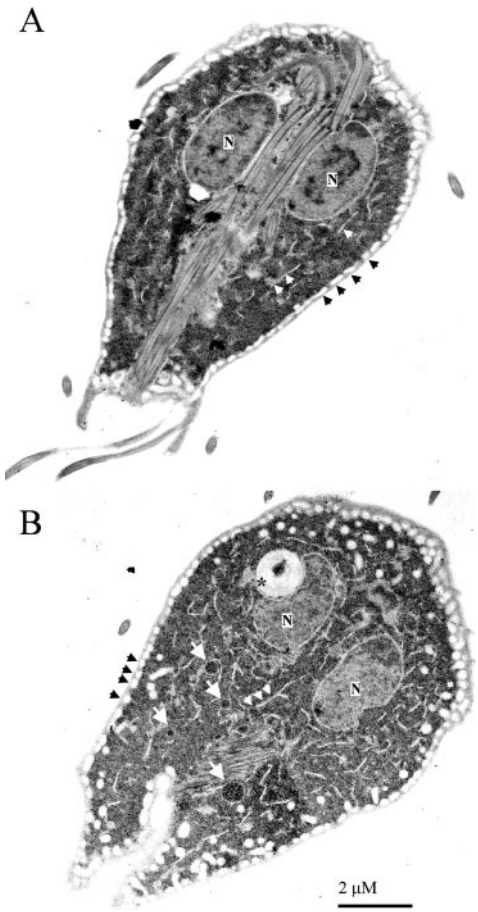

FIG. 1. **Anatomy of the *Giardia* endomembrane system: a tEM survey.** All cells were sectioned parallel to the ventral plane. *A*, normal trophozoite with distinct nuclear envelope/ER compartments extending bilaterally from the nuclei to the posterior end of the cell body. *B*, encysting cell (11 h postinduction of encystation) showing the emergence of ESVs. The ER cisternae appeared dilated and the distribution of PVs changed slightly, but no distinct vesicular compartments resembling a Golgi apparatus were detectable in both developmental stages. Abbreviations and symbols: *N*, nucleus; *small white arrowheads*, endoplasmic reticulum; *black arrowheads*, PVs; *white arrows*, ESVs; *asterisk*, perinuclear spindle-shaped structure. *Scale bar* is 2 μm.

genomic search for members of these gene families in the *Giardia* HTGS data base. These included sequences coding for subunits of the COPI, COPII, and adaptor protein (AP) coat complexes, the SNARE family of tethering factors and their corresponding adaptors, which belong to the Sec1 family, the Rab GTPases and, finally, the large vesicle tethering complexes Sec34/35 and VPS52/53/54 and the exocyst complex, which are organized in three gene families.

By pairwise reciprocal BLAST searching of the *Giardia* Genome Data base for subunits we identified genes coding for five of seven postulated *Giardia* COPI subunits α-, β-, β′-, δ-, and ζ-COP (Table I). A *Giardia* γ-COP subunit has not been identified yet, and ϵ-subunits are not sufficiently conserved to be identified with BLAST searches. We also identified all COPII subunits, *i.e.* the complete ORFs of two *Giardia* Sec24 paralogues, Gisec24a and GiSec24b, as well as the *Giardia* orthologues of Sec23, Sec13, and Sec31 (Table I). Two complete sets of heterotetrameric *Giardia* AP subunits (Table I) were also found using subunits from AP-1 to AP-4 from *Homo sapiens* and *Arabidopsis thaliana*, or AP-1 to AP-3 from *S. cerevisiae* as query sequences. A re-Blast of the *Giardia* HTGS data base with these eight putative AP subunits as query sequences did not reveal additional hits, making the existence of a third AP complex in *Giardia* highly unlikely. Consequently, *Giardia* is the first organism examined to date with only two putative AP complexes. Furthermore, we identified an orthologue of the clathrin heavy chain in the genome (Table I), termed GiCLH. The putative ORF encodes a 1871-amino acid protein with three (*S. cerevisiae*: seven) C-terminal clathrin repeats and one N-terminal propeller, according to a Pfam analysis. Not surprisingly, identification of a clathrin light chain in the *Giardia* genome was not successful, presumably because clathrin light chain orthologues share exceedingly low sequence homology.

A *Giardia ARF* gene homologue has been cloned and sequenced previously (29) and was used to rescue a lethal yeast mutant (30). In this study we identified ORFs predicting three additional members of the ARF family in *Giardia* (Table I). Phylogenetic analysis (data not shown) suggests that one protein belongs to the same subgroup as ARF (ARF2), whereas the two other proteins comprise the *Giardia* ARL subgroup (ARL1 and ARL2). We also found a predicted related *Giardia* Sar1p protein to be highly homologous to the corresponding *A. thaliana* orthologue (Table I).

Specific factors on acceptor membranes and transport vesicles confer specificity to fusion events and are therefore critical for maintaining organelle integrity. These include the membrane-associated SNARE family of proteins and the small Rab GTPases, which act as molecular switches.

SNAREs comprise a family of related integral membrane proteins that mediate a variety of membrane docking and fusion reactions in eukaryotic cells. The family of SNARE proteins can be divided into Q-SNAREs with a conserved central glutamine residue (syntaxin and SNAP subgroups) and R-SNAREs with a conserved central arginine residue (vamp/synaptobrevin subgroup), whereby three Q-SNAREs and one R-SNARE are required for the action of a functional tetrameric helical bundle. In our attempts to identify *Giardia* orthologues of members of the two SNARE subclasses we validated initial BLAST results using the Pfam tool to confirm the presence of conserved structural syntaxin (Syn) or synaptobrevin (Vamp) domains. In a first round of data base searches we uncovered four putative *Giardia* SNAREs (Table I): two Q-SNAREs (GiSyn1 and GiSyn4) and two R-SNAREs (GiVamp1 and GiVamp2). Using these *Giardia* SNARE orthologues as query sequences, we found an additional syntaxin-like Q-SNARE with closest homology to GiSyn1 (termed GiSyn2, Table I). The presence of predicted C-terminal transmembrane domains in GiSyn1, GiSyn2, GiSyn4, and GiVamp2 and a C-terminal prenylation site in GiVamp1 further supported the correct identification of these SNARE orthologues. The cytosolic Sec1 proteins interact directly with members of the syntaxin subfamily of SNAREs. A previous phylogenetic analysis of members of the Sec1 family of proteins (31) revealed that of the four Sec1 members in yeast, Sec1p, Sly1p, and VPS45p belong to one subgroup, and VPS33p constitutes a second subgroup. Additional gene duplications in *Caenohrabditis elegans* and human have only been observed with *Sec1p*. *Giardia* seems to contain only two Sec1 paralogues, a prototypic GiSec1p and second Sec1 paralogue most closely related to the yeast VPS33 protein (GiVPS33p, Table I).

Rab GTPases are molecular switches cycling between an active, membrane-associated, GTP-bound and an inactive, cytosolic, GDP-bound state. Because different Rabs preferentially localize to distinct vesicles and organelles in their activated state, they are assumed to be critical for the specificity of membrane fusion. Our genomic survey revealed eight genes coding for Rab proteins in *Giardia* (Table I). These include orthologues of *Rab1* (*GiRab1*) and *Rab11* (*GiRab11*), with high homology to the corresponding proteins in *S. cerevisiae*, *C. elegans*, and *H. sapiens,* and two orthologues of *Rab2*

TABLE I
Translated putative Glardia orthologues

Putative *Giardia* orthologue	Length (aa)	Organism	Closest homologue: protein accession No.	% Id[a]	% Sim[b]	BLAST P(n) e^{-c}	Pfam P(n) e^{-}	Pfam domain
GiCLH	1871	*H. sapiens*	NP_004850.1	24	41	140	4	Clathrin
Adaptor protein subunits								
Glγ adaptin[e]	347	*Ustilago maydis*	CAA86825.1	30	47	24	18	AP large
Giα adaptin[e]	288	*Neurospora* crassa	CAB98218.1	33	53	35	26	AP large
Giβa adaptin[e]	672	*H. sapiens*	NP542150.1	25	48	32	7	AP large
Giβb adaptin[e]	1132	*H. sapiens*	NP001273.1	35	53	92	69	AP large
Giμa adaptin[e]	448	*Dictyostelium discoideum*	AAG11391.1	24	45	29	12	AP medium
Giμb adaptin[e]	434	*Dictyastelium discoideum*	AAH41282.1	33	52	72	114	AP medium
Gia adaptin[e]	141	*A. thaliana*	NP_175219.1	61	82	40	62	AP small
Gib adaptin[e]	147	*Mus musculus*	XP_129915.1	39	54	22	25	AP small
COPI subunits								
Giα-COP[f]	1277	*Aspergillus nidulans*	AAC18088	26	41	85	11	WD40
Giβ-COP[f]	1017	*C. elegans*	NP_494441	35	54	15	17	AP large
Giβ'-COP[e]	1003	*A. thaliana*	NP_188219	24	42	49	8	WD40
Giδ-COP[f]	523	*Zea mays*	AF216852_1	27	44	2	7	AP medium
Giζ-COP[f]	159	*Glycine max*	BAA92779	31	46	2	2	AP small
COPII subunits								
GiSec13p[f]	294	*A. thaliana*	AC010676_2	25	44	12	4	WD40
GiSec23p[f]	860	*D. melanogaster*	AAF51978	32	49	120	70	PB02188/Sec23
GiSec24a[f]	804	*A. thaliana*	AC012395_23	24	40	36	16	PB02576/Sec24
GiSec24b[f]	980	*H. sapiens*	NP_006314	22	38	15	9	PB02576/Sec24
GiSec31p[f]	1024	*S. cerevisiae*	NP_010086	25	44	7	4	WD40
Rab/ARF GTPases								
GiRab1[g,k]	212	*Oryza sativa*	BAB07961	59	76	56	87	Ras
GiRab2a[g,k]	214	*Z. mays*	AAA63901	61	75	64	87	Ras
GiRab2b[g]	227	*Gallus gallus*	2209256A	56	73	58	84	Ras
GiRabD[e]	204	*Entamoeba histolytica*	AF389109_1	31	47	20	18	Ras
GiRabF[e]	271	*H. sapiens*	S72399	41	60	30	25	Ras
GiRabA[e]	192	*M. musculus*	AF408432_1	27	47	10	13	Ras
GiRabBt[e]	185	*M. musculus*	XP_126820	36	57	26	13	Ras
GiRab11[g]	216	*Discopyge ommata*	P22129	56	75	48	74	Ras
GiARF1[h]	191	*O. sativa*	BAB90396	71	85	75	125	ARF
GiARF2[g]	166	*A. thaliana*	NP_179133	40	56	29	47	ARF
GiARL1[g]	179	*Xenopus laevis*	AAL77055	50	74	47	68	ARF
GiARL2[f]	197	*D. melanogaster*	ARL2_DROME	44	68	41	70	ARF
GiSar1p[e]	191	*O. sativa*	BAB63877	48	65	46	56	ARF
SNARE/Sec1								
GiSyn1[i]	307	*C. elegans*	BAA23584	21	44	13	4	t-SNARE
GiSyn2[i]	271	*C. elegans*	NP_498105	22	42	7	6	Syntaxin
GiSyn4[j]	293	*H. sapiens*	XP_012569	40	58	0.4	4	Syntaxin
GiVamp1[e]	209	*Candida albicans*	CAA21982	28	49	16	6	PB0957 Syn.brevin
GiVamp2[f]	210	*Schizosacchoromyces pombe*	CAB39850	25	46	13	6	PH00957 Syn.brevin
GiSec1[f]	847	*M. musculus*	BAA19478	21	39	6	3	Sec1
GiVPS33[b,f]	641	*Rattus norvegicus*	AAC52985	22	39	16	9	Sec1

[a] Id, percent Identity.
[b] %Si; percent similarity.
[c] P (n) e; negative logarithm of expect value.
[d] Protein sequences based on a partial ORF.
[e] Identified and posted to GenBank on in this study.
[f] Identified in this study and subject to confirmation.
[g] Posted to GenBank™ previously by N. Iwabe (unpublished data).
[h] Identified and characterized by Murtagh *et al.* (29).
[i] Identified by Dacks and Doolittle (54).
[j] Posted to GenBank™ previously by Touz *et al.*, unpublished data.
[k] Identified by Langford *et al.* (53).

(*GiRab2a* and *GiRab2b*). In various organisms, Rab1/2 and Rab11 have well characterized functions in anterograde transport from ER to Golgi and in cycling of vesicles from endosomes to the TGN or exit from the TGN, respectively. In addition, we identified four highly diverged *Giardia* Rab homologues, *GiRabA/B/D/F*, whose identities could not be assigned with confidence based on sequence homology alone. However, all four of these highly diverged *Giardia* GTPases show highest similarity to the five functional Rab domains (RabF1–5 as defined by Ref. 32) rather than to the corresponding domains of the Ras/Rho/Arf groups within the superfamily of Ras proteins.

Three recently identified multisubunit protein complexes are involved in vesicle tethering at distinct trafficking steps in yeast and human cells. The COG complex (33) (formerly termed Sec34/35 complex (34)) is involved in intra-Golgi recycling and recycling from endosomes back to the Golgi (35). Four of the eight COG subunits are structurally and phylogenetically related with each other and share sequence homology with four subunits of the exocyst and two of the GARP complex. The exocyst (36) is a complex associated with the TGN in yeast and mammalian cells and is involved in trafficking to the plasma membrane, mostly at sites of polarized secretion. The GARP complex (formerly termed VPS52/53/54 (37)) is required for retrograde transport from endosomes to the TGN. Surprisingly, our survey indicated that *Giardia* lacks each of these complexes. We were unable to identify any subunits of these

quatrefoil complexes involved in vesicle tethering during trafficking to and from the TGN. The conspicuous absence of these factors adds molecular support to the hypothesis that a conventional Golgi is not present in this protozoan.

The Secretory Machinery Components Are Not Stage Specifically Expressed in Giardia—Encystation causes significant morphological changes of the endomembrane system of *Giardia*, notably the appearance of discrete ER exit sites followed by the apparent neogenesis of large ESVs. If ESVs indeed corresponded to a Golgi, and are generated *de novo*, this developmental induction of a compartment structure should be reflected in changes of steady-state mRNA levels of the broad panel of markers and complexes detailed in Table I. To address this question and to identify markers potentially associated with the developmentally regulated genesis of ESV compartments, we performed a semiquantitative RT-PCR analysis and compared mRNA levels in trophozoites with those in parasites in an early phase of encystation *in vitro* (7 h postinduction). Message levels of only one representative subunit gene of each COPI, COPII, and putative API/II complex were measured. As a positive control for encystation, we determined induction of endogenous *CWP1* transcripts. mRNA levels of the constitutively expressed protein phosphatase 2 (*PP2*) (16) were determined as a control that equal amounts of cDNA were being compared. Cycle numbers for PCR amplification were adapted to individual cDNA levels to allow densitometric quantification of each pair of SYBR green-stained PCR products (trophozoites/cells 7 h postinduction of encystation) within the linear range of the Fluoroimager detection filter. Semi-quantitative RT-PCR of 24 different mRNAs and densitometric analysis revealed no or only minor changes in transcript levels during stage conversion (Figs. 2, *A* and *B*). In comparison with the mRNA coding for the CWP1 protein (~90-fold induction), mRNA levels of the analyzed markers were only very moderately elevated in encysting cells, if at all. The levels of six of these weakly induced mRNAs (*GiSec24a*, *GiRab2a*, *GiRabA*, *GiRab11*, *GiSar1*, and *GiVPS33*) were determined more precisely at five time points during the encystation process (trophozoites, 3/7/15/24 h postinduction of encystation) by Light Cycler PCR™ (Fig. 2*C*), using *PP2* mRNA as the constitutive standard. *GiRabF* was not analyzed further despite some indications of up-regulation in encysting cells because of the extremely low levels of steady-state mRNA. This approach confirmed the modest induction levels of certain mRNAs (*GiSec24a*, *GiRabA*, and *GiRab2a*), and demonstrated that none of the secretory components investigated in this study were induced only during encystation.

Generation of Polyclonal Antibodies Against Seven "Sentinel" Proteins and Analysis of Compartment Dynamics during Encystation—Using comparative genomics, we showed that *Giardia* holds the basic machinery constituting a eukaryotic secretory system, and that the major components of this machinery were not stage-regulated. To analyze stage-specific dynamics of the *Giardia* secretory system in more detail, we generated a novel set of antibodies against selected proteins predicted to be associated with different components and compartments of this apparatus. These pAbs were used as tools in a systematic investigation of the membrane compartments anatomy in *Giardia* and specifically, to address the question whether some of these sentinel proteins were involved in the generation and/or maintenance of ESVs. As a key criterion for the latter, we addressed the question whether some of these marker proteins re-localized to ESVs from cytoplasmic pools or other membrane compartments during encystation. The markers used in this investigation were: GiSar1p, Giβ′COP, GiCLH, GiSyn1, and GiRab11 (see also Table I). Two additional and separately identified proteins were included: (i) a *Giardia* orthologue of the yeast dynamin-like protein VPS1p (38) termed GiDLP; (ii) GiYip, a homologue of the recently identified protein Yip1p in yeast, which interacts with the transport GTPase Ypt1p at the Golgi (39). Mouse antisera against fusion proteins or the GiDLP peptide were analyzed for specificity by Western blot using total protein from vegetatively dividing trophozoites. All antibodies detected a major band that corresponded to the molecular mass of the predicted proteins (Fig. 3*A*).

The seven pAbs were used to localize the corresponding marker proteins within the *Giardia* cytoplasm and/or endomembrane system by immunofluorescence assay (IFA), and to determine its dynamics during encystation and ESV formation. A mAb against a cyst wall protein was used as an internal marker to label cyst wall material in ESVs. Specific pAbs against GiSar1p-labeled nuclear envelope membranes and the clamp-shaped ER compartment in both developmental stages (Fig. 4*A*) but not ESVs. Co-localization of CWP and GiSar1p was occasionally detected in areas where ER exit sites had been found previously (18). GiSyn1, a *Giardia* syntaxin homologue, did not re-localize to ESV membranes at all, but remained associated with internal and peripheral membrane structures in both developmental stages (Fig. 4*D*). In contrast, the putative *Giardia* COPI coat complex, represented by the Giβ′COP subunit, partially redistributed to ESVs during stage conversion (Fig. 4*B*). Interestingly, the antibody labeled as yet uncharacterized structures in trophozoites as well. Because COPI is associated exclusively with Golgi membranes in all eukaryotes, this was the first direct evidence for the existence of a putative Golgi-like organelle in *Giardia* trophozoites. Similarly, GiRab11 exhibited ESV labeling in encysting cells in addition to the peripheral distribution observed in trophozoites (Fig. 4*E*). GiYip was mostly confined to punctate structures along the clamp-shaped reticular ER in trophozoites and encysting cells, reminiscent of ER exit sites (18), and partially localized to ESV membranes (Fig. 4*F*). GiCLH was detected exclusively in close association with PVs in trophozoites at the periphery of the cell body, and re-localized to ESVs in late encysting cells only (18). GiDLP showed a similar distribution with two major differences: (i) in trophozoites the marker was distinctly associated with PVs but also other internal structures, and (ii) in contrast to GiCLH, antibodies against GiDLP already labeled early, immature ESVs and the marker remained associated with these compartments until secretion of the cyst wall material. The results showed that the seven markers investigated here were expressed in both trophozoites and encysting cells and thus provided independent confirmation of the semi-quantitative RT-PCR experiment. Moreover, we showed that this set of antibodies including the anti-CWP mAb can be used to distinguish the three known membrane compartments ER, PVs, and ESVs. Finally, the IFA data showed that the markers, which partially (Giβ′COP, GiYip, and GiRab11) or mostly (GiCLH and GiDLP) redistributed to ESVs during encystation, localized to distinct compartments in trophozoites. This supported the notion that the vesicular transport system in *Giardia* is constitutive and argued against the hypothesis that ESVs are *de novo* generated compartments.

Trophozoites Contain a Compartment with Golgi Characteristics—Clear identification of endomembrane compartments using IFA experiments remained difficult because of the very limited information available on the structure of the *Giardia* endomembrane system. We used subcellular fractionation techniques in conjunction with this novel set of antibodies as a complementary approach to improve compartment characterization, and to investigate the stage-specific dynamics of the secretory apparatus. In particular, we were interested if marker proteins that were seen to associate with ESVs by IFA

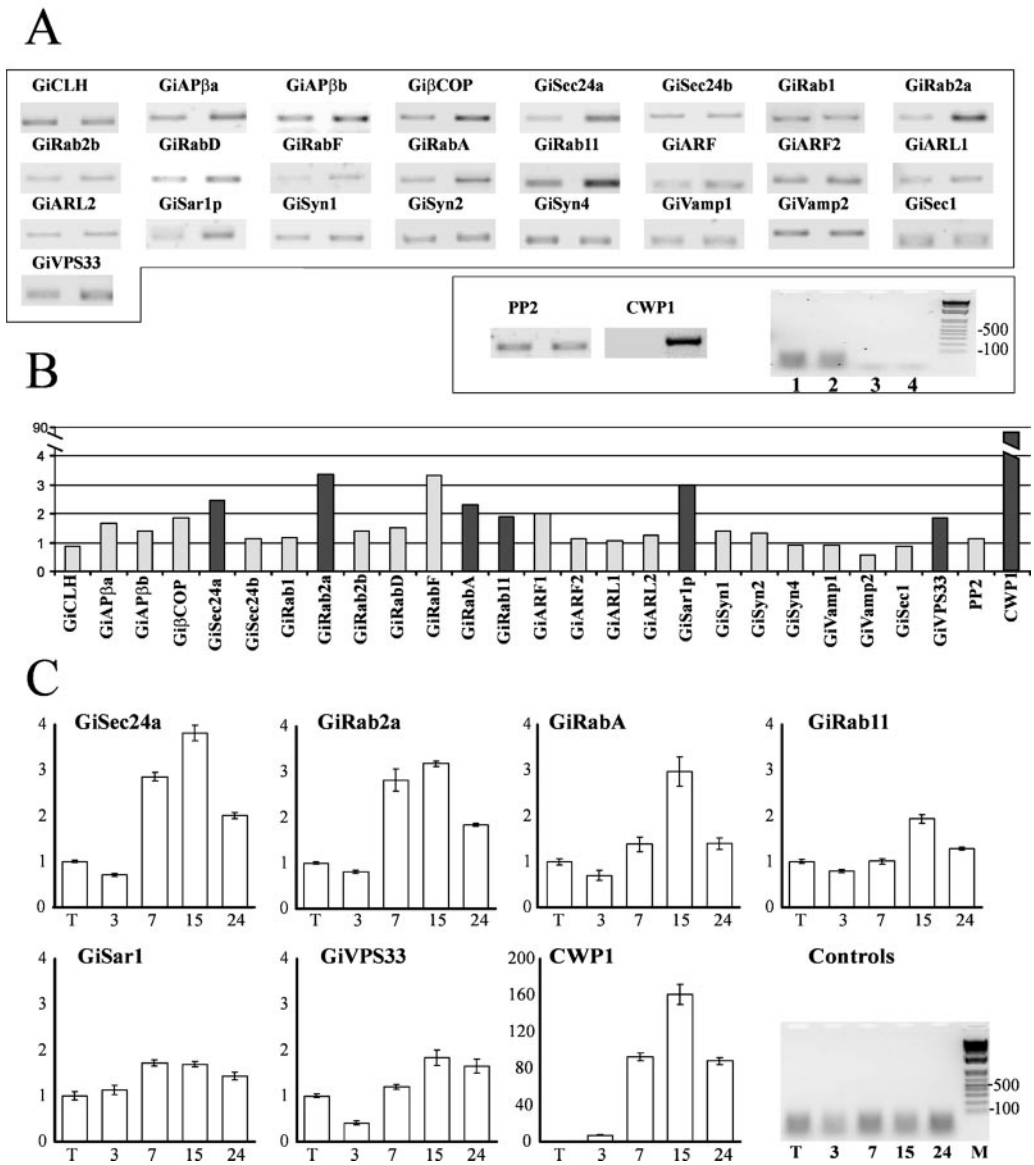

FIG. 2. **Transcriptional dynamics of secretory apparatus components during stage-conversion.** *A*, semi-quantitative PCR analysis. Equal amounts of total RNA from trophozoites and encysting cells (7 h postinduction of encystation) were used to generate single-stranded cDNA by RT-PCR. Gene-specific products amplified from cDNA of trophozoites (*left lane*) and encysting cells (*right lane*) were separated on agarose gels and stained with SYBR green. *Inset* in *A*, controls. *PP2* represents a constitutive gene used as loading control, and *CWP1* represents an induced gene used to monitor encystation efficiency. Negative controls were used for semi-quantitative PCR. (i) Omission of template cDNA using gene-specific primers of *PP2* (*lane 1*) and *CWP1* (*lane 2*). (ii) Omission of enzyme in the RT-PCR reaction using RNA from trophozoites (*lane 3*) or encysting cells (*lane 4*). *B*, diagrammatic representation of induction factors as a proportion of transcription levels in encysting cells and trophozoites, respectively, from *A*. Single bands have been quantified densitometrically. *Gray bars*, genes with an induction factor below 2. *Black bars*, genes with an induction factor of 2 or higher. *C*, light cycler analysis. Equal amounts of total RNA from trophozoites and encysting cells (3, 7, 15, and 24 h postinduction of encystation) were used to generate single-stranded cDNA by RT-PCR. Negative controls, PCR amplification after cDNA synthesis with omission of RT using the primer pair to amplify the PP2 RACE product. Note that *GiRabB* is missing in *panel A* because it is not expressed in either stage and may be a pseudogene, based also on its atypical C terminus.

were recruited from cytoplasmic pools or compartments with completely different characteristics in trophozoites, as predicted if ESVs were indeed a novel Golgi-like compartment. Using the antibodies described above we first demonstrated that we could indeed reproducibly generate and separate distinct microsome populations from trophozoites and encysting cells with a dynamic range between sucrose densities of 20 and 55%. Sucrose gradients were eluted into 18 fractions of equal volume after centrifugation and proteins were separated on SDS-PAGE and blotted to nitrocellulose membranes. We showed that detection of marker proteins with specific antibodies resulted in distinct distribution profiles (Fig. 5), reflecting the association of the markers with microsomes of defined densities, or the presence of the marker as a soluble protein in the cytoplasm (*e.g.* the cytoplasmic pool of GiSar1p). Each profile was verified in at least three fractionation experiments; densitometric analysis of a representative experiment was used for graphical presentation of Western blot data in Fig. 5*B*. A representative Western blot reflecting the subcellular distribution of GiDLP in both developmental stages is shown in Fig. 5*A*. ESV-derived microsomes prepared from encysting cells were identified using a mAb against the cargo protein CWP1 (fractions 10–12). The lack of soluble CWP in the top fractions (cytoplasm) demonstrated the faithful resealing of ESVs during the cell disruption process. The peak of the Golgi marker Giβ′COP overlapped significantly (fractions 11 to 13) with those of the Golgi-associated GlcNAc-transferase enzyme activity and CWP at a sucrose concentration of 22 to 26%. Similar

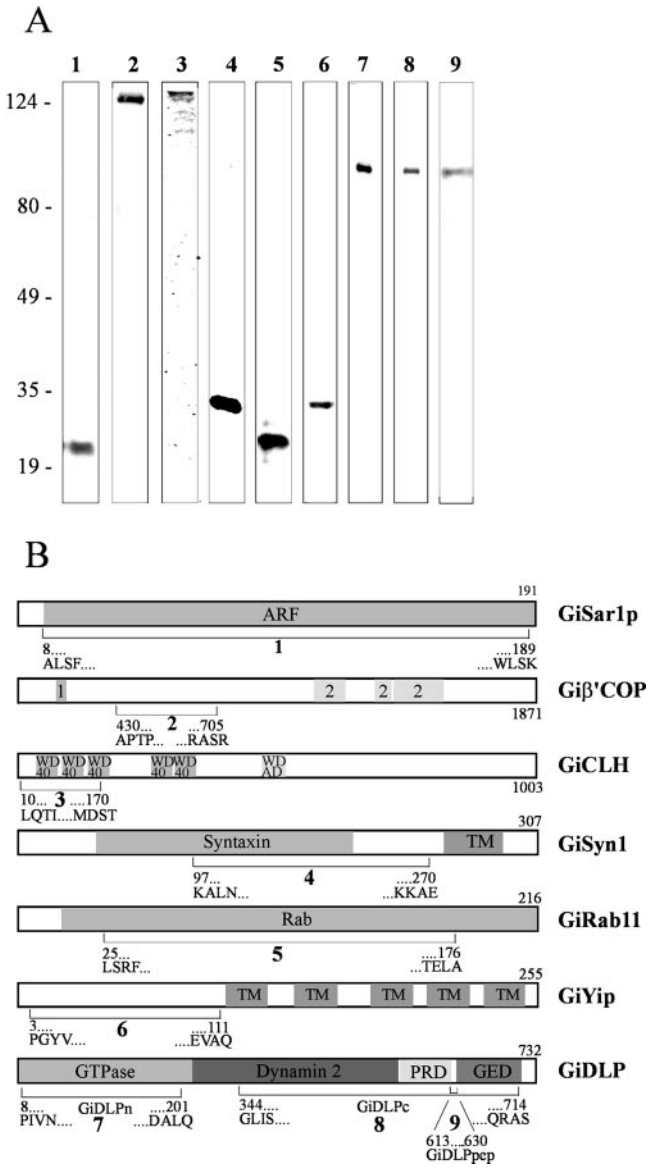

FIG. 3. **Sentinel proteins used for IFA and subcellular fractionation.** *A*, Western blot analysis. Total trophozoite lysates were separated by SDS-PAGE and blotted to nitrocellulose membranes. *Lanes 1–6* represent GiSar1 (*lane 1*, predicted mass: 21 kDa), Giβ'-COP (*lane 2*, predicted mass: 112 kDa), GiCLH (*lane 3*, predicted mass: 205 kDa), GiSyn1 (*lane 4*, predicted mass: 34 kDa), GiRab11 (*lane 5*, predicted mass: 24 kDa), GiYip (*lane 6*, predicted mass: 28 kDa), GiDLPn (*lane 7*, predicted mass: 80 kDa), GiDLPc (*lane 8*), and GiDLPpep (*lane 9*). Relative molecular masses (M_r) of size markers are indicated. *B*, diagrammatic representation of the seven sentinel proteins based on prediction of structural domains and transmembrane regions using Pfam and PSORTII software (for URLs see footnotes). *Numbers* on *top* of each *bar* denote the total number of amino acids. *Numbers* and *letters below* the *brackets* indicate amino acid position and corresponding one-letter code, respectively, encompassing the protein portions used for antibody production. *Bold numbers* correspond to numbering of immunoblots in *A*. Abbreviations: *WD40*, WD-40 repeat; *TM*, transmembrane domain; *PRD*, proline-rich domain; *GED*, GTPase effector domain. *Numbers* representing domains in GiCLH: *1*, N-terminal propeller domain; *2*, C-terminal clathrin repeat.

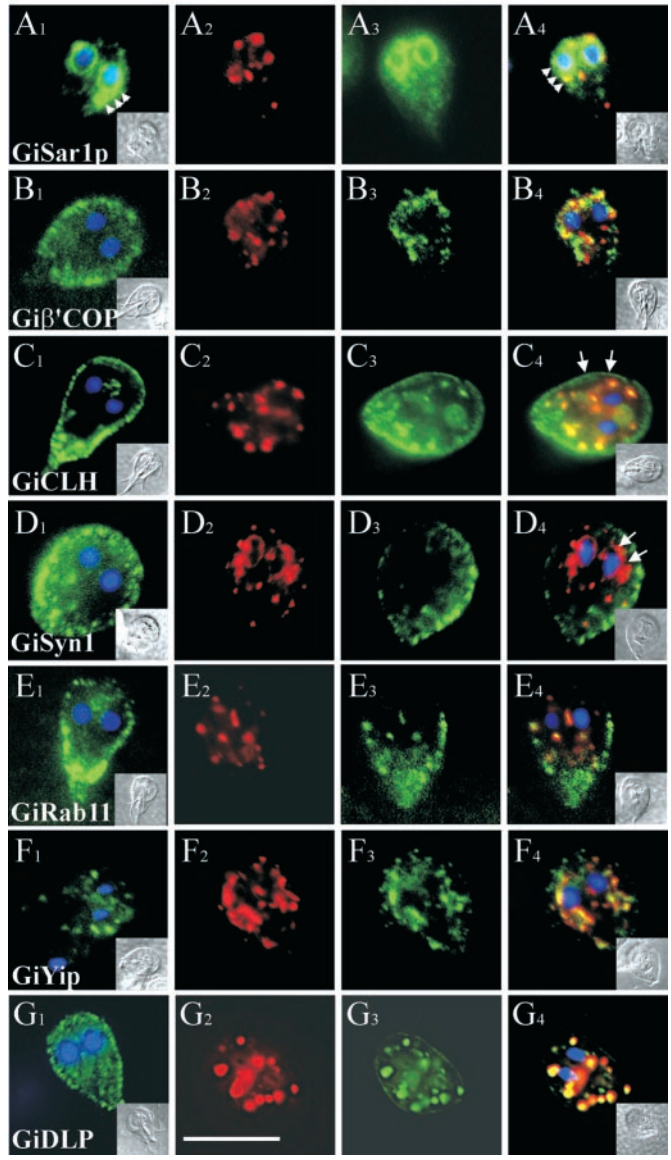

FIG. 4. **Subcellular localization of marker proteins by IFA.** Mouse antibodies to recombinant proteins were used to localize the marker proteins in formaldehyde-fixed and detergent-permeabilized trophozoites. *A1–G1*, merged 4,6-diamidino-2-phenylindole and FITC images of a trophozoite cell; the marker antibody was detected with a secondary anti-mouse FITC conjugate. *A2–G2*, CWP1 in an encysting cell detected with CWP1-TR conjugated mouse antibody. *A3–G3*, merged 4,6-diamidino-2-phenylindole and FITC (marker antibody, see above) images of an encysting cell. *A4–G4*, merged image of 4,6-diamidino-2-phenylindole/FITC and CWP1. *Small insets* in *columns 1* and *4*, differential interference contrast image. Note: GiSar1 specifically localizes to the clamp-shaped ER structure (*white arrowheads*); Giβ'COP, GiCLH, GiYip, GiRab11, and GiDLP partially or completely co-localize to ESVs with CWP1 (merge in *column 4*); GiCLH (*white arrows*) and GiDLP specifically label ESVs and PVs, whereas GiSyn1 does not co-localize with CWP1 (*white arrows*). *Scale bar* is 10 μm.

density values have also been reported in initial fractionation studies for the purification of ESVs (17) and of Golgi microsomes in mammalian systems (40). The five sentinel proteins (Giβ'COP, GiCLH, GiYip, GiDLP, and GiRab11), which localized to ESVs by IFA in encysting cells also showed a major peak at sucrose concentrations between 25 and 29%, whereas the GiSyn1 peak (6–9) did not overlap with CWP-containing fractions. Most importantly, Giβ'COP, GiYip, GiDLP, and GiRab11, as well as GlcNAc-transferase activity, were also associated with microsomes from trophozoites with identical densities. This showed for the first time that membrane-bound compartments with characteristics equivalent to those of ESVs were present in trophozoites. Consistent with IFA data, the trophozoite GiCLH peak did not overlap with the peak generated by the ESV-associated clathin. Three markers (GiCLH, GiDLP, and GiSyn1) showed a second peak at densities similar to those reported for lysosomes (40–44%) or, alternatively, microsomes derived from rough ER (38–54%) of higher eu-

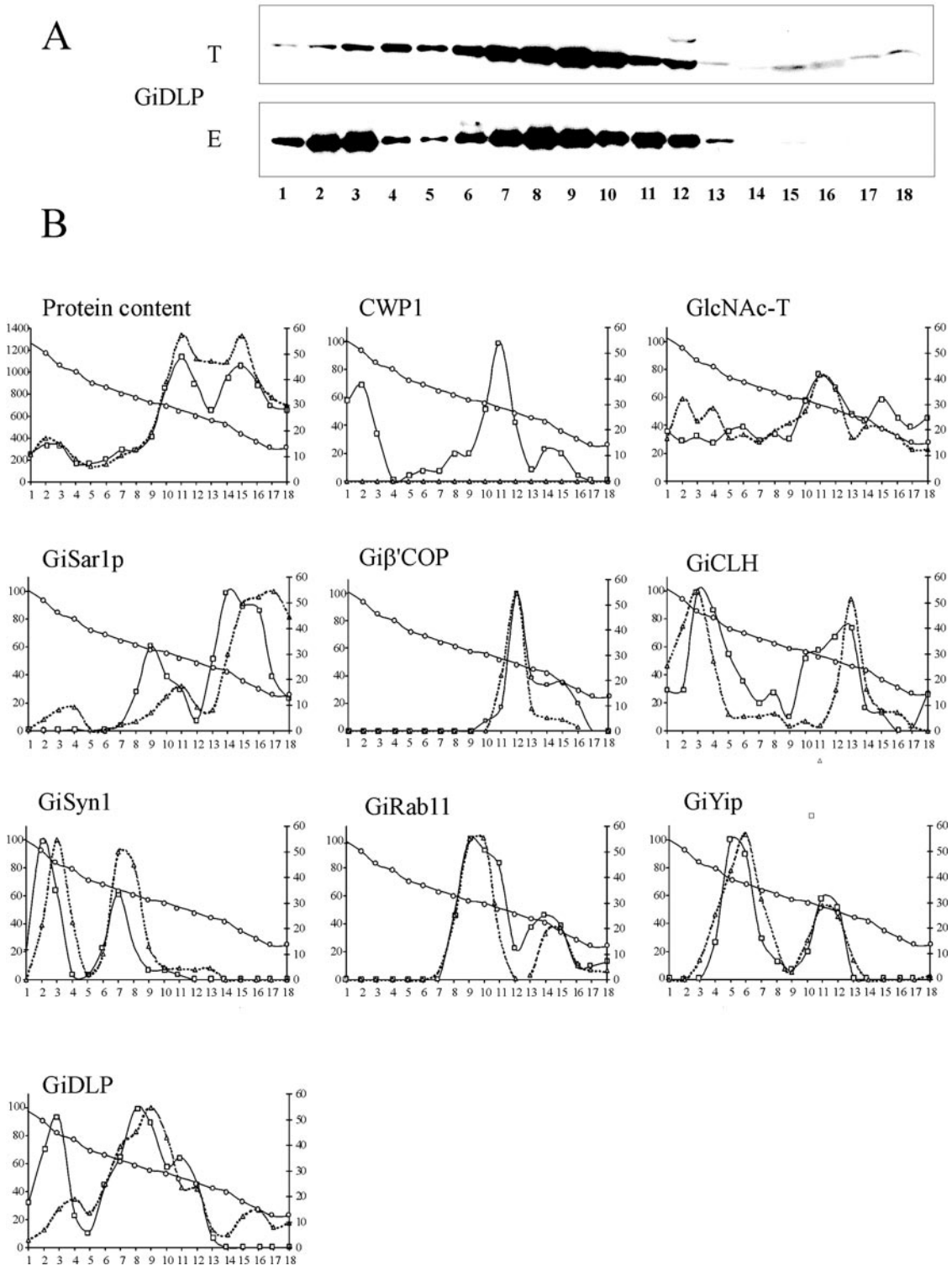

FIG. 5. **Distribution of marker proteins by subcellular fractionation.** Postnuclear supernatants of *Giardia* trophozoites and encysting cells were fractionated on sucrose gradients. Fractions were collected from bottom (fraction 1) to top (fraction 18). *A*, representative Western blot analysis showing the subcellular distribution of GiDLP in trophozoites (*T*) and encysting cells (*E*). *B*, densitometric quantification of immunoblots (exemplified by GiDLP in *A*). Total enzymatic activity or maximal densitometric values in the gradient were set to 100%; protein content is indicated in micrograms/ml. Shown is the distribution of CWP (internal ESV marker), GlcNAc-transferase activity, GiSar1p, Giβ'COP, GiCLH, GiSyn1, GiRab11, GiYip, and GiDLP. *Dashed line* (△), trophozoites; *solid line* (□), encysting cells; *solid line* (○), sucrose concentrations (% w/v).

karyotes (40). Considering the observed localizations in IFA experiments we favor the interpretation that these markers are associated with PVs, which apparently have similar densities as reported for lysosomes, but we cannot exclude association of GiDLP with ER-derived microsomes during encystation (fractions 1–3). Microsomes derived from the ER usually peak at two densities in fractionation studies of other eukaryotic cells: a rough ER fraction with a significantly higher density than Golgi microsomes, and a smooth ER fraction, which may overlap with the Golgi microsomes (40). The extensive *Giardia* ER is likely to be organized in distinct subdomains (including ER exit sites, which sometimes appear as punctate structures

TABLE II
Interpretation of IFA and subcellular fractionation

Synthesis of subcellular fractionation and IFA datasets indicating localization of markers used in this study.

Marker protein	Interpretation
CWP1	ER, ESV
GISar1p	ER, CP
Giβ′COP	ESV/Golgi, CP
GiCLH	ESV/Golgi, PV, CP
CiYip	ER, ESV
GiSyn1	PV,?
GiRab11	ESV/Golgi, (PV?),[a] CP
GiDLP	ESV/Golgi, PV, CP,?
GicNAc-T[b]	ESV/Golgi

[a] GiRab11 localized to peripheral structures reminiscent of PVs by IFA but had no corresponding PV peak in subcellular fractionation experiments (Fig. 5*B*).

[b] Compartment distribution of GlcNAc-trausferase was determined by subcellular fractionation only.

in IFA (18)), and may even be directly connected to PVs (41, 42). IFA data showed that GiSar1p evenly localized to the clamp-shaped ER/nuclear envelope membranes. This is in agreement with the GiSar1 peaks detected in fractions 3, 4, and 9–12 (8–11 in encysting cells), whereas the large peak in fractions 14–18 represents the cytoplasmic pool. GiYip is a predicted integral membrane protein and showed a punctate distribution along the ER structure in IFA. Its distribution is correspondingly different to that of GiSar1p with only a minor overlap (fractions 10 and 11) and no cytoplasmic pool. Finally, a third peak in the subcellular distribution of GiCLH, GiDLP, and GiSyn1 between 30 and 36% sucrose (fractions 6–8) could not be assigned to a specific compartment with confidence. The variety of profiles obtained by different markers indicated a more complex anatomy of the *Giardia* endomembrane system than tEM studies would suggest. All markers except GiSyn1 and GiYip are peripheral membrane proteins, which cycle between a cytoplasmic and a compartment-bound state. It is therefore important to note that these proteins have sometimes large cytoplasmic pools, represented by a peak in fractions at the top of the gradient.

A synthesis of the combined IFA and subcellular fractionation data indicating the localization(s) of marker proteins is presented in Table II. Note that IFA images of encysting cells are representative but, as opposed to the subcellular fractionation data, cannot reflect the variations among the population. The subcellular fractionation data show a virtual lack of major shifts in peak localization and relative size between preparation from trophozoites and encysting cells (Fig. 6, Table II). The few exceptions (*i.e.* GiDLP and GiSar1p) concern peaks in fractions denser than ESVs and will have to be investigated further. The remarkably similar profiles obtained in both developmental stages again supported the existence of compartments in trophozoites that are biochemically related to ESVs. Together with the fact that mRNA expression levels of the major secretory pathway components including several Golgi marker proteins were not stage-specifically regulated, the data presented here argued against a previously postulated hypothesis that Golgi structure and function are induced only during encystation in *Giardia* (17) and are not present in proliferating trophozoites.

DISCUSSION

The evolution of the eukaryotic endomembrane system represents one of the key events in the transition from prokaryotes to eukaryotes. To understand the workings of the complex machineries involved in secretory transport of higher eukaryotes, it is of major interest to investigate early-diverged species, which may harbor an ancient and thus minimal apparatus for the ordered transport of proteins and lipids during

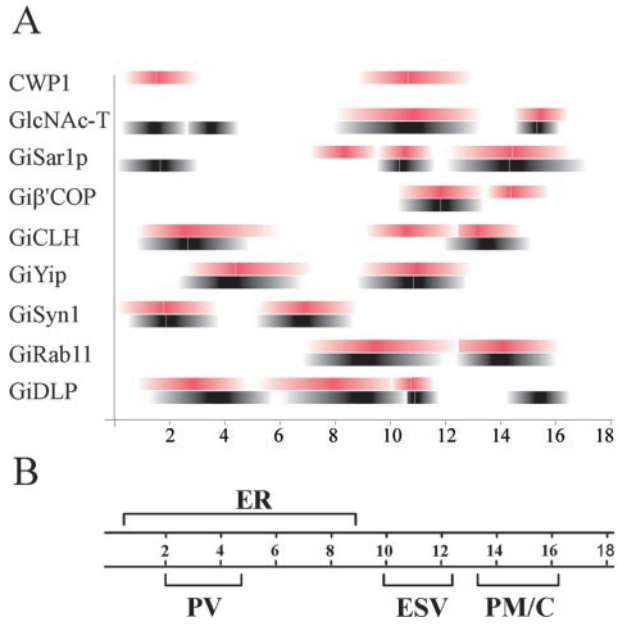

FIG. 6. **Representation of combined results from IFA and SF.** *A*, graphical depiction of the subcellular distribution data from Fig. 5. Peaks are represented by maximum intensity of the *horizontal bars*. Note the rather subtle changes in the distribution of markers between the two developmental stages. *Gray bars*, trophozoites; *red bars*, encysting cells. *B,* interpretation of the combined data. *PM/C*, plasma membrane and/or cytoplasmic pool.

growth and development. The diplomonads as the most basal eukaryotes known to date may shed light on some of these developments. For example, certain groups suggested that *Giardia* has no membrane structures resembling a Golgi apparatus, whereas others have claimed to detect the classical multicisternal membrane arrangement in EM studies (25, 43). In agreement with the former, we recently showed that sorting of cargo proteins to the regulated ESV or the constitutive VSP pathways occurred at or immediately after export from the ER during encystation (18). Others have provided data suggesting that Golgi structure and function were induced only during encystation in the form of ESVs (17), organelles that collect and transport cyst wall material to the nascent extracellular matrix. In a tEM survey using a novel method for preparing adhering *Giardia* for analysis we found no evidence for conventional Golgi stacks in a single parasite. Most encysting cells contained a large spindle-shaped membrane structure (up to 2 μm) adjacent to one or both nuclei that had been interpreted as Golgi stacks in earlier EM investigations of randomly sectioned cells (43), but resembled "karmellae" from higher eukaryotes (*i.e.* layers of proliferated ER membranes wrapped around the nucleus (44)).

The absence of large Golgi stacks, or even Golgi "ministacks" as observed in *Pichia pastoris* (45) is evidence for an unconventional membrane transport system, but not proof that a functional Golgi does not exist in *Giardia*. Although morphological evidence could not be found, we demonstrated that on a molecular genetic level *Giardia* holds the basic modules constituting a classical eukaryotic secretory apparatus. Identification of a molecular framework for secretory transport in *Giardia* allowed to significantly extend insights from a recent study on eukaryotic membrane compartment organization based on genome sequence data from *S. cervisiae*, *C. elegans*, *Drosophila melanogaster*, and *H. sapiens* (26) (Table III). Our data implies an increase in complexity from the ancestral *Giardia* "core system" to its yeast counterpart similar to that from single cells (*S. cerevisiae*) to multicellular organisms (*C. elegans*). For ex-

TABLE III
Secretory apparatus components in Giardia and higher eukaryotes
Presence and number of gene families involved in vesicular transport in *Giardia* and higher cukaryotes (this study and Refs. 26 and 28).

	Giardia	*S. cerevisiae*	*C. elegans*	*H. sapiens*
COP complexes	2	2	2	2
AP complexes	2	3	3	4
Rabs	8	11	29	60
SNAREs	5	23	26	39
Sec1s	2	4	5	6
Quatrefoil complex[a]	None	3	3	3

[a] Includes the three quatrefoil tethering complexes GARP, COG, and exocyst.

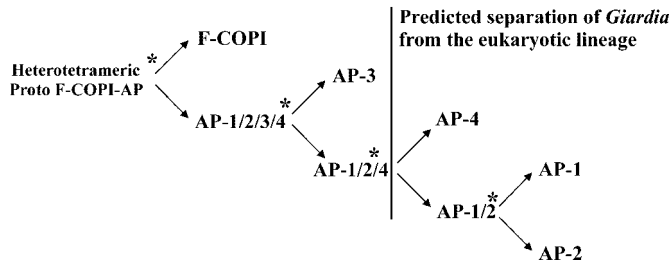

FIG. 7. **Point of separation of *Giardia* from the eukaryotic lineage based on AP evolution.** The *graph* illustrates the current hypothesis on the evolution of the four AP complexes and the F-COPI subcomplex through successive rounds of coordinated gene duplications (*) (27, 52). The *vertical bar* indicates the predicted point of separation of *Giardia* from the other eukaryotic lineages.

ample, we identified only a limited number of factors involved in ordered fusion of membrane vesicles in *Giardia*: three Q-SNAREs and two R-SNAREs (*S. cerevisiae*: 23, *C. elegans*: 26), and eight paralogues of the Rab protein family (*S. cerevisiae*: 11, *C. elegans*: 29). Interestingly, preliminary phylogenetic analysis of AP subunits (data not shown) supported the presence of only two putative AP complexes in *Giardia*, AP-I and AP-II. According to the current model on the evolution of AP complexes by a series of coordinated gene duplications (27), the two prototypic *Giardia* AP complexes predicted the point of separation of *Giardia* (*i.e.* the diplomonads as a whole) after the first coordinated round of gene duplications resulting in an AP-3 and an AP1/2/4 ancestor (Fig. 7). Based on the *Giardia* orthologues and functional categories identified in this study, one can specify the secretory apparatus of the last common ancestor of diplomonads and the eukaryotic lineage. Such a hypothetical ancestral secretory apparatus would consist of four vesicle coat complexes (two AP-clathrin complexes, COPI and COPII), six or seven Rab proteins (assuming group-specific gene duplications of the closely related GiRab2a/b), two SNARE complexes, and two corresponding SNARE adaptors of the Sec1 family.

Because the developmental induction of Golgi structure and function had been postulated previously, it was of interest to test whether the expression of any of the now uncovered structural components of the secretory machinery in *Giardia* was regulated or constitutively active. The lack of significant expression regulation of the genes investigated (Fig. 2) provided important evidence that the *Giardia* secretory system is not subject to stage-regulation during encystation on a molecular level, even though this was surprising considering the significant morphologic changes in membrane structures. In particular, the steady-state mRNA levels of *Giardia Rab* and *SNARE* family members were more stable than expected. In *Trypanosoma brucei*, for example, the Golgi-associated TbRab18 protein (46), or the endocytic TbRab11 (47) and coat components such as the clathrin heavy chain or APβ1 (48), are developmentally regulated, in response to changes in Golgi functions or the different requirements for endocytotic traffic in bloodstream forms or procyclic stages, respectively. With respect to the idea that ESVs are Golgi cisternae, the transcriptional analyses suggested, that even though ESVs were novel structures by morphological criteria they may not be generated *de novo*, but correspond in their basic biochemical characteristics to hitherto unidentified Golgi-like compartments in trophozoites. Additional independent support for the latter came from results obtained with IFA and subcellular fractionation experiments. A set of seven novel antibodies against marker proteins was used as sentinels to investigate the dynamics of the *Giardia* endomembrane system during a developmental transition where major morphological changes could be observed accompanying the emergence of ESVs. In addition to the detection of major compartments, some unexpected and novel structures were recognizable whose exact nature will have to be determined in future investigations. Most significantly, the presence and association of all marker proteins with specific subcellular compartments in trophozoites indicated the existence of a constitutive transport system, and presumably some form of Golgi apparatus. The most interesting finding of the complementing cell fractionation experiments was the detection of a microsome population with the same density as ESVs rather than a "vesicle gap," as would have been predicted if there was no Golgi-like compartments in trophozoites. This was unexpected considering the previous absence of any morphological and biochemical evidence for a Golgi in trophozoites (17, 18), an idea that was also based on an earlier study where GlcNAc-transferase activity was detected only in encysting cells but not in trophozoites (17). Other data (49) and our own showed practically identical GlcNAc-transferase activity levels (peaks in fractions 10–12) in trophozoites and encysting parasites (10 h postinduction), however. These results indicating a constitutive Golgi structure and function also agreed with reports that export of VSPs to the plasma membrane in trophozoites was sensitive to brefeldin A (17), suggesting coatomer-dependent transport processes to the cell surface in trophozoites. How does this fit with previous models (18), which feature ESVs as the only secretory compartments with Golgi characteristics? The unique nature of ESVs as transient Golgi-like compartments is because of their conspicuous morphology, their defined cargo, and their stability over a period of several hours. Functionally similar compartments in trophozoites (and presumably throughout the life cycle) evidently lack this stability and are bound to be difficult to identify because of this. Therefore, the existing models will have to be adapted to feature two Golgi-like systems, which exist simultaneously, at least in encysting cells. In addition to different degrees of stability, these parallel systems presumably have unique cargo specificities as already suggested in previous work (18). Because protein sorting appears to occur at a pre-Golgi level, the exported cargo itself may ultimately determine the functional identity of the compartment in which it will travel to its destination. These compartments will therefore display specific biochemical characteristics, *e.g.* making pre-Golgi vesicles containing CWP cargo selectively fusion competent, or mature ESVs receptive for the exocytosis signal. In trophozoites, the current data suggest that VSPs are exported through a direct pathway with fast kinetics to the plasma membrane. This pathway is brefeldin A-sensitive but VSPs, or similarly targeted reporters, are insubstantially modified by post-translational processes (50), if at all, in agreement with the hypothesis that their export involves passage through a constitutive short-lived Golgi-like organelle. Consequently, the simplest (and probably too simplistic) scenario would predict that the comparatively long-lived ESVs could be generated from a constitutive apparatus by

recruitment of only one or few factors, which mediate homotypic fusion of ER-derived transport intermediates and stabilize the nascent cisternae for the time until exocytosis, without the complex neogenesis of an entire secretory system. Considering the important role such putative factors play during stage conversion, their identification and characterization will be key to understanding the principles for generation and maintenance of Golgi-like cisternae in *Giardia*, and perhaps in general. This model is consistent with a specialized "pulse-chase" version of the cisternal maturation model (51): (i) ESVs are generated from smaller pre-Golgi vesicles by homotypic fusion; (ii) ESVs mature by retrograde transport via COPI-coated vesicles; (iii) mature ESVs are analogous to single-cargo trans Golgi cisterna and associated with clathrin; (iv) ESVs disperse simultaneously into small secretory vesicles that fuse with the plasma membrane and release their contents.[6]

The results presented here indicate novel aspects concerning possible Golgi functions in the context of a primordial secretory system in this basal protozoan. The evidence we now find for such structures in trophozoites makes the *Giardia* model system more consistent, because the previously postulated *de novo* synthesis of Golgi cisternae had been difficult to explain. All the challenging questions remain, *i.e.* how are cargo proteins sorted during export, and to what extent do their targeting signals determine the nature and fate of transport vesicles. In addition, we will start looking for factors responsible for the selective stabilization of ESVs. These molecules will provide the answer to the question, how early eukaryotes maintained Golgi cisternae for extended periods of time and evolved mechanisms for maturation and controlled secretion of more extensively modified cargo.

Acknowledgments—Human fibroblasts (cell line MRC-5, ATCC number CCL 171) were a kind gift of Dr. Peter Deplazes. We gratefully acknowledge the excellent technical assistance of Dr. Marianne Bienz and Therese Michel. We are indebted to the people of the Giardia Genome Project for sharing their sequence data.

REFERENCES

1. Brugerolle, G. (1974) *Protistologica* **10,** 83–90
2. Brugerolle, G., Kunstyr, I., Senaud, J., and Friedhoff, K. T. (1980) *Z. Parasitenkd.* **62,** 47–61
3. Eyden, B. P., and Vickerman, K. (1975) *J. Protozool.* **22,** 54–66
4. Sogin, M. L., Gunderson, J. H., Elwood, H. J., Alonso, R. A., and Peattie, D. A. (1989) *Science* **243,** 75–77
5. Leipe, D. D., Gunderson, J. H., Nerad, T. A., and Sogin, M. L. (1993) *Mol. Biochem. Parasitol.* **59,** 41–48
6. Hashimoto, T., Sanchez, L. B., Shirakura, T., Muller, M., and Hasegawa, M. (1998) *Proc. Natl. Acad. Sci. U. S. A.* **95,** 6855–6860
7. Roger, A. J., Svard, S. G., Tovar, J., Clark, C. G., Smith, M. W., Gillin, F. D., and Sogin, M. L. (1998) *Proc. Natl. Acad. Sci. U. S. A.* **95,** 229–234
8. Horner, D. S., and Embley, T. M. (2001) *Mol. Biol. Evol.* **18,** 1970–1975
9. Benchimol, M., Ribeiro, K. C., Mariante, R. M., and Alderete, J. F. (2001) *Eur. J. Cell Biol.* **80,** 593–607
10. Morgado-Diaz, J. A., Nakamura, C. V., Agrellos, O. A., Dias, W. B., Previato, J. O., Mendonca-Previato, L., and De Souza, W. (2001) *Parasitology* **123,** 33–43
11. Soltys, B. J., Falah, M., and Gupta, R. S. (1996) *J. Cell Sci.* **109,** 1909–1917
12. Knodler, L. A., Noiva, R., Mehta, K., McCaffery, J. M., Aley, S. B., Svard, S. G., Nystul, T. G., Reiner, D. S., Silberman, J. D., and Gillin, F. D. (1999) *J. Biol. Chem.* **274,** 29805–29811
13. McCaffery, J. M., Faubert, G. M., and Gillin, F. D. (1994) *Exp. Parasitol.* **79,** 236–249
14. Adam, R. D. (2001) *Clin. Microbiol. Rev.* **14,** 447–475
15. Reiner, D. S., McCaffery, M., and Gillin, F. D. (1990) *Eur J. Cell Biol.* **53,** 142–153
16. Hehl, A. B., Marti, M., and Kohler, P. (2000) *Mol. Biol. Cell* **11,** 1789–1800
17. Lujan, H. D., Marotta, A., Mowatt, M. R., Sciaky, N., Lippincott-Schwartz, J., and Nash, T. E. (1995) *J. Biol. Chem.* **270,** 4612–4618
18. Marti, M., Li, Y., Schraner, E. M., Wild, P., Kohler, P., and Hehl, A. B. (2003) *Mol. Biol. Cell* **14,** 1433–1447
19. Boucher, S. E., and Gillin, F. D. (1990) *Infect. Immun.* **58,** 3516–3522
20. McArthur, A. G., Morrison, H. G., Nixon, J. E., Passamaneck, N. Q., Kim, U., Hinkle, G., Crocker, M. K., Holder, M. E., Farr, R., Reich, C. I., Olsen, G. E., Aley, S. B., Adam, R. D., Gillin, F. D., and Sogin, M. L. (2000) *FEMS Microbiol. Lett.* **189,** 271–273
21. Hehl, A. B., Lekutis, C., Grigg, M. E., Bradley, P. J., Dubremetz, J. F., Ortega-Barria, E., and Boothroyd, J. C. (2000) *Infect. Immun.* **68,** 7078–7086
22. Lujan, H. D., Mowatt, M. R., Conrad, J. T., Bowers, B., and Nash, T. E. (1995) *J. Biol. Chem.* **270,** 29307–29313
23. Wild, P., Schraner, E. M., Adler, H., and Humbel, B. M. (2001) *Microsc. Res. Tech.* **53,** 313–321
24. Vischer, P., and Hughes, R. C. (1981) *Eur. J. Biochem.* **117,** 275–284
25. McCaffery, J. M., and Gillin, F. D. (1994) *Exp. Parasitol.* **79,** 220–235
26. Bock, J. B., Matern, H. T., Peden, A. A., and Scheller, R. H. (2001) *Nature* **409,** 839–841
27. Schledzewski, K., Brinkmann, H., and Mendel, R. R. (1999) *J. Mol. Evol.* **48,** 770–778
28. Whyte, J. R., and Munro, S. (2001) *Dev. Cell* **1,** 527–537
29. Murtagh, J. J., Mowatt, M. R., Lee, C. M., Lee, F. J., Mishima, K., Nash, T. E., Moss, J., and Vaughan, M. (1992) *J. Biol. Chem.* **267,** 9654–9662
30. Lee, F. J., Moss, J., and Vaughan, M. (1992) *J. Biol. Chem.* **267,** 24441–24445
31. Tellam, J. T., James, D. E., Stevens, T. H., and Piper, R. C. (1997) *J. Biol. Chem.* **272,** 6187–6193
32. Pereira-Leal, J. B., and Seabra, M. C. (2001) *J. Mol. Biol.* **313,** 889–901
33. Ungar, D., Oka, T., Brittle, E. E., Vasile, E., Lupashin, V. V., Chatterton, J. E., Heuser, J. E., Krieger, M., and Waters, M. G. (2002) *J. Cell Biol.* **157,** 405–415
34. Lupashin, V. V., Pokrovskaya, I. D., McNew, J. A., and Waters, M. G. (1997) *Mol. Biol. Cell* **8,** 2659–2676
35. Whyte, J. R., and Munro, S. (2002) *J. Cell Sci.* **115,** 2627–2637
36. TerBush, D. R., Maurice, T., Roth, D., and Novick, P. (1996) *EMBO J.* **15,** 6483–6494
37. Conibear, E., and Stevens, T. H. (2000) *Mol. Biol. Cell* **11,** 305–323
38. Rothman, J. H., Raymond, C. K., Gilbert, T., O'Hara, P. J., and Stevens, T. H. (1990) *Cell* **61,** 1063–1074
39. Yang, X., Matern, H. T., and Gallwitz, D. (1998) *EMBO J.* **17,** 4954–4963
40. Bonifacino, J. S., Dasso, M., Harford, J. B., Lippincott-Schwartz, J., and Yamada, K. M. (eds) (2001) *Current Protocols in Cell Biology*, Vol. 1.2, John Wiley and Sons, Inc., New York
41. Touz, M. C., Nores, M. J., Slavin, I., Carmona, C., Conrad, J. T., Mowatt, M. R., Nash, T. E., Coronel, C. E., and Lujan, H. D. (2002) *J. Biol. Chem.* **277,** 8474–8481
42. Lanfredi-Rangel, A., Attias, M., de Carvalho, T. M., Kattenbach, W. M., and De Souza, W. (1998) *J. Struct. Biol.* **123,** 225–235
43. Lanfredi-Rangel, A., Kattenbach, W. M., Diniz, J. A., Jr., and de Souza, W. (1999) *FEMS Microbiol. Lett.* **181,** 245–251
44. Wright, R., Basson, M., D'Ari, L., and Rine, J. (1988) *J. Cell Biol.* **107,** 101–114
45. Rossanese, O. W., Soderholm, J., Bevis, B. J., Sears, I. B., O'Connor, J., Williamson, E. K., and Glick, B. S. (1999) *J. Cell Biol.* **145,** 69–81
46. Jeffries, T. R., Morgan, G. W., and Field, M. C. (2002) *Mol. Biochem. Parasitol.* **121,** 63–74
47. Jeffries, T. R., Morgan, G. W., and Field, M. C. (2001) *J. Cell Sci.* **114,** 2617–2626
48. Morgan, G. W., Allen, C. L., Jeffries, T. R., Hollinshead, M., and Field, M. C. (2001) *J. Cell Sci.* **114,** 2605–2615
49. Das, S., and Gillin, F. D. (1996) *Exp. Parasitol.* **83,** 19–29
50. Marti, M., Li, Y., Kohler, P., and Hehl, A. B. (2002) *Infect. Immun.* **70,** 1014–1016
51. Allan, B. B., and Balch, W. E. (1999) *Science* **285,** 63–66
52. Boehm, M., and Bonifacino, J. S. (2001) *Mol. Biol. Cell* **12,** 2907–2920
53. Langford, T. D., Silberman, J. D., Weiland, M. E., Svard, S. G., McCaffery, J. M., Sogin, M. L., and Gillin, F. D. (2002) *Exp. Parasitol.* **101,** 13–24
54. Dacks, J. B., and Doolittle, W. F. (2001) *Cell* **107,** 419–425

[6] M. Marti and A. B. Hehl, unpublished data.

Supplementary Table:
Primers used for RT-PCR and semi-quantitative PCR
Lower case letters designate restriction enzyme recognition sites.

k-anchor	5'-CCGgaattcGGTACCtctaga(T_{18})K-3'
k-adaptor	5'-CCGgaattcGGTACCtctaga-3'
CWP1-s-q	5'-CTGGTACATGAGTGACAACGCT-3'
PP2-s-q	5'-CACGTTGGGAGACCATTGCA-3'
GiCLH-s-q	5'-TTGGCCTGGGTCAACAGAATG-3'
GiAPβa-s-q	5-AGCCTCTTCTCCACCACAATATAAC-3
GiAPβb-s-q	5-AAACTTCAACCTCGTGGAAATG-3
GiβCOP-s-q	5-TGAGAGGCTTGTCTGATACTTC-3
GiSec24a-s-q	5-AAACAGCTATCTCCCCATATTC-3
GiSec24b-s-q	5-ACAGCCCGTGGAATAAG-3
GiRab1-s-q	5-GATCTCTTTCATCGAAAC-3
GiRab2a-s-q	5'-AGGAGGCGTTCATGATAATTG-3'
GiRab2b-s-q	5'-ACCACGGCCTTCTCTTCATC-3'
GiRabD-s-q	5'-CGCCAACAGTTGATGTTCAAG-3'
GiRabF-s-q	5'-GTAATTATAGCAGGCCAGATAC-3'
GiRabA-s-q	5'-GACTCTCCGATATTCTTCATTTG-3'
GiRab11-s-q	5'-AGCAAGGCCTTTCGTACATTG-3'
GiARF-s-q	5'-AAGAAGCGCGACTGGTATATC-3'
GiARF2-s-q	5'-GCCAACAAGCAGGACATAGAC-3'
GiARL1-s-q	5'-TGGTGTCCCCATTCTAGTTTTC-3'
GiARL2-s-q	5'-CTTCTCTCGGAGCTCCTTATC-3'

GiSar1p-s-q 5’-TATTCTCATCCTGAGCAACAAG-3’

GiSyn1-s-q 5’-CAGCAGAGCAGACTAATTGAAC-3’

GiSyn2-s-q 5’-GGAACGGTGCTAGATAGAATAG-3’

GiSyn4-s-q 5’-CGAACCAGGAGACGATCAAC-3’

GiVamp1-s-q 5’-

AAGAGAACGATCAGCTTTCTAAG-3’

GiVamp2-s-q 5’-ACTCGCGCAAAGGACATAATG-

3’

GiSec1-s-q 5’-CAGAGCCCAGTCCGTTCAAC-3’
GiVPS33-s-q 5’-TCAGTGCTCGTGGTCTTTATTG-3’

2. Primers used for antibody production

GiβCOP-EcoRI-s 5-CGgaattcCTTCAGACCATCCGCACATC-3

GiβCOP-PstI-as 5-AAActgcagGATGGACTCTACAATCAAAGCGTAA-3

GiSar1p-EcoRI-s 5-CGgaattcAAGTCGGCACTGTCTTTTC-3

GiSar1p-PstI-as 5-ATCctgcagTTACTTGGAGAGCCACTTAAAAC-3

GiCLH-BamHI-s 5-CGggatccGCACCAACGCCAATCATGATC-3’

GiCLH-PstI-as 5’-ATCctgcagTTAGCGCGATGCACGTTTGATATAC-3’

GiRab11-EcoRI-s 5’-CGgaattcTCGAGGTTCACCAGCAACAAG-3’

GiRab11-PstI-as 5’-AAActgcagTTAGGCTAGTTCAGTAACGAGCTG-3’

GiSyn1-EcoRI-s 5’-CGgaattcGCACTAAACACGCAAATCCAAG-3’

GiSyn1-PstI-as 5’-AAActgcagTTACTCCGCCTTCTTTAAGTAAGTTG-3’

GiDLPn-EcoRI-s 5’-CGgaattcCCGATTGTCAACTCCTTGCAG-3’

GiDLPn-PstI-as 5’-AAActgcagTTATGCGTCAGAAGTTGCGAGATC-3’

GiDLPc-EcoRI-s 5’-CGgaattcGGGCTCATATCCTCCTACGAG-3’

GiDLPc-PstI-as	5’-ATCctgcagTTAGCTTGCGCGTTGCATAACATC-3’
GiYip1p-EcoRI-s	5’-GCgaattcCCAGGCTATGTTGGTGATGAC-3’
GiYip1p-XbaI-as	5’-GCtctagaTTACTGCGCAACTTCGTCTGAG-3’

An Ancestral Secretory Apparatus in the Protozoan Parasite *Giardia intestinalis*

Matthias Marti, Attila Regös, Yajie Li, Elisabeth M. Schraner, Peter Wild, Norbert Müller, Lea G. Knopf and Adrian B. Hehl

J. Biol. Chem. 2003, 278:24837-24848.
doi: 10.1074/jbc.M302082200 originally published online April 23, 2003
